Standardization of ^{18}F by Means of $4\pi(\mathrm{PS})\beta - \gamma$ Plastic Scintillator Coincidence System

Aída M. Baccarelli, Mauro S. Dias, Marina F. Koskinas, and Franco Brancaccio

***Abstract*—The present work describes the procedure developed for the standardization of ^{18}F by means of a coincidence system using a plastic scintillator detector in 4π geometry, named $4\pi(\mathrm{PS})\beta - \gamma$, which was developed at the Nuclear Metrology Laboratory in IPEN, São Paulo, Brazil. The main advantage of this detector system is the ability to perform primary standardizations without the need for a coating of a metal layer on the radioactive source film for rendering it conductive, as usually necessary for proportional counter measurements. The measurements were also performed with a conventional $4\pi(\mathrm{PC})\beta-\gamma$ coincidence system, which makes use of a 4π proportional counter for charged particles or X-ray detection coupled to a pair of NaI(Tl) scintillation counters. The gamma-ray window was set to measure the 511 keV gamma-rays produced by positron annihilation. The detector efficiency was changed by moving the electronic discriminator threshold. The observed activity values were extrapolated to 100% efficiency and the results showed good agreement between the two detector systems.**

***Index Terms*—Coincidence, fluorine-18, plastic scintillator, standardization.**

I. Introduction

RADIONUCLIDE calibration systems applying $4\pi\beta - \gamma$technique have been considered primary standards for many years due to high accuracy and because the results depend only on observable quantities (see for instance: [1]–[7]). The Nuclear Metrology Laboratory (Laboratório de Metrologia Nuclear, LMN) of IPEN (Instituto de Pesquisas Energéticas e Nucleares) has recently developed a $4\pi(\mathrm{PS})\beta - \gamma$ coincidence system, which makes use of a plastic scintillator as a charged particle detector in 4π geometry [8], [9]. This detector is intended to perform primary standardizations using thin Collodion films as radioactive source holder. However, since this system is based on light collection instead of gas ionization, it is not necessary to use any metal layer coating on the radioactive source film in order to render it conductive. In the present work, ^{18}F was chosen for testing this system. This is a very important radionuclide to radiopharmacy, especially for Positron Emission Tomography (PET) applications.

The ^{18}F decay scheme is shown in Fig. 1. This radionuclide has a 1.8290(5) h half-life and decays by β^+ emission with 96.80(20)% probability and electron capture with 3,20(20)% probability. The maximum β^+ energy is 633.5(6) keV [10]. This radionuclide has been standardized previously at the LMN by a conventional $4\pi\beta(\mathrm{PC}) - \gamma$ coincidence system employing a gas flow proportional counter, as part of an International comparison organized by the National Physical Laboratory, UK, in 2001 [11].

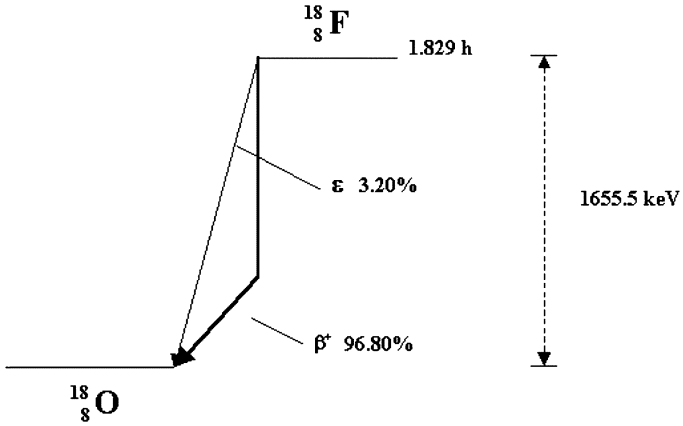

Fig. 1. Decay scheme of ^{18}F.

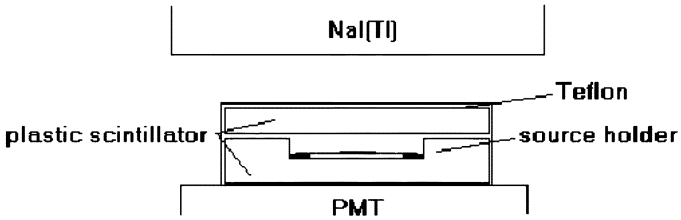

Fig. 2. Coincidence system using 4π plastic scintillator coupled to a NaI(Tl) crystal.

II. Experimental Procedure

A. Description of the $4\pi(PS)\beta - \gamma$ System

The geometry of the 4π plastic scintillator coincidence system is shown in Fig. 2. More details are given elsewhere [8], [9]. It consists of a double plastic cylindrical scintillator in which the lower part is 6 mm thick and has a coaxial depression of 3 mm where the radioactive source is placed. The upper part is 3 mm thick and is used as a lid to improve light collection efficiency and to assure 4π geometry. The scintillator was wrapped with Teflon tape for producing diffused light reflection. The lower end was coupled to a RCA 8850 photomultiplier tube by means of silicone grease. A similar system is described in [12], where the radioactive solution is deposited

Manuscript received February 23, 2007; revised March 10, 2008.

A. M. Baccarelli is with the Departamento de Fisica, 111 CEP 01303-050 São Paulo, Brazil (e-mail: aida@lvk.com.br).

M. S. Dias, M. F. Koskinas, and F. Brancaccio are with the Nuclear Metrology Laboratory, CRPq/Nuclear Physics Division, Instituto de Pesquisas Energéticas e Nucleares, 05508-000 São Paulo, Brazil (e-mail: msdias@ipen.br; koskinas@ipen.br; fbrancac@ipen.br).

Digital Object Identifier 10.1109/TNS.2008.921492

directly on the plastic scintillator. In the present system, the source is supported by a Collodion film, therefore it can be removed to be used for calibration in other primary systems such as $4\pi(\mathrm{PC})\beta-\gamma$. This procedure was performed in the present work, as described in the following sections.

The lower discrimination level was initially set to 6 keV in order to cut off noise. Further measurements were performed by moving to upper levels in order to change the β efficiency. The whole set was coupled to a 76 mm $\times$ 76 mm NaI(Tl) scintillator counter for gamma ray detection. The gamma channel window was set to include only the total absorption peak produced by ^{18}F annihilation gamma rays. A single NaI(Tl) detector was employed in this experiment, therefore only one gamma ray could be detected per annihilation pair. Typical beta ray counting rates from source and background were 1000 and 25 cps, respectively. The corresponding rates for gamma rays were 52 and 4 cps, respectively.

B. Description of the $4\pi(PC)\beta-\gamma$ Reference System

The system used as [5] consisted of a gas-flow proportional counter with 4π geometry using 90% Ar +10% CH_4 gas at 0.1 MPa, as the β detector, coupled to a pair of 76 mm $\times$ 76 mm NaI(Tl) scintillation counters as γ detectors. The proportional counter was operated with +2050 V bias. The lower discrimination level was initially set to 60 mV and then moved to upper levels in order to change the β efficiency. Monte Carlo simulations of the 4π detector geometry were performed using code PENELOPE [13] showing that the peak in the beta spectrum corresponds to a deposited energy around 3 keV in the gas. Therefore, the adopted lower level threshold corresponds to an energy around 0.1 keV. This value is much lower than the ^{18}F Auger electron energy. The gamma channel window was set to include only the total absorption peak produced by ^{18}F annihilation gamma rays. Since the two NaI(Tl) crystals were positioned at opposite sides with respect to 4π detector, some events summed up and were removed from the gamma-ray window. Typical beta ray counting rates from source and background were around 1000 and 2 cps, respectively. The corresponding rates for gamma rays were around 100 and 7 cps, respectively.

C. Positron Spectrum in the $4\pi(\mathrm{PS})$ Detector

The ^{18}F positron spectrum is shown in Fig. 3. The left part of the spectrum corresponds to pulses coming from the upper half of the scintillator and the right part corresponds to pulses coming from the lower half of the scintillator. This gain mismatch between the two scintillator halves does not represent a problem because this detector is used only for integral counting and not as a spectrometer. The shape in the low amplitude region indicates that many low energy positrons produce pulses in the noise region. As a result the maximum positron efficiency for ^{18}F is lower than that in a 4π proportional counter.

D. Electronic System

The electronic system diagram is shown in Fig. 4. This system eliminates the need of individual counters for each detection line. In addition, contribution from accidental coincidences can

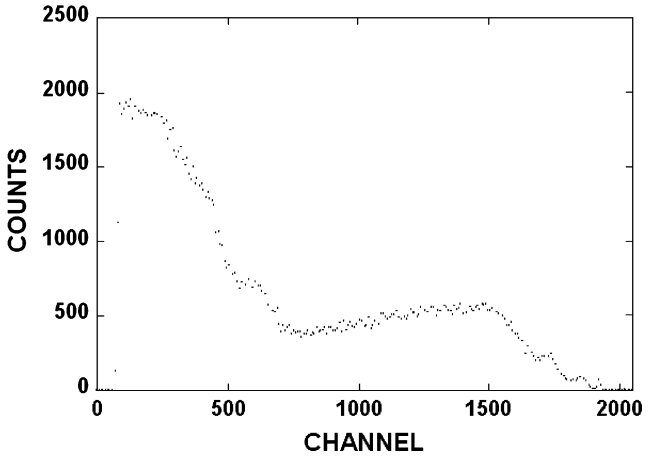

Fig. 3. Positron spectrum from the $4\pi(\mathrm{PS})$ detector. The left part of the spectrum corresponds to pulses coming from the upper half of the scintillator and the right part corresponds to pulses coming from the lower half of the scintillator.

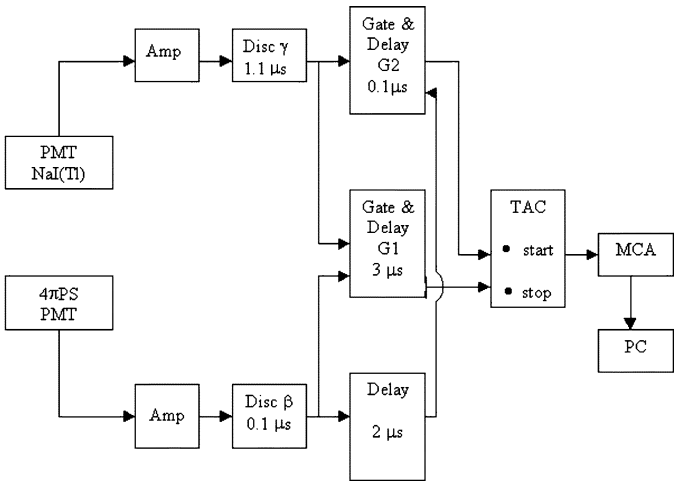

Fig. 4. Schematic diagram of electronic system.

be determined experimentally by means of the time distribution registered by the system.

In the first step the pulses pass through an amplifier having 0.5 μs shaping time. The resulting timing signal at the amplifier output occurs 1.8 μs after disintegration. Next, the pulses are discriminated by means of Single Channel Analysers (SCA). The first SCA was set to cut off noise from the plastic scintillator. The second one was used for the gamma ray window chosen to accept only total energy absorption pulses from 511 keV ^{18}F annihilation quanta.

The logic pulses were sent to gate and delay modules, then to a Time to Amplitude Converter (TAC) Ortec Model 567 and finally to a Multichannel Analyser (MCA) Camberra Model S400 Genie-PC Spectroscopy System. The TAC module operated with 5 μs full scale and the MCA operated with 2048 channels. Signals from both β and γ lines fed the same Gate and Delay generator G2 but at different times due to the presence of a delay module placed in the β line. As a result, the starting signals from β and γ events occur at different times at the TAC start input. The Gate and Delay generator G1 was set to 3 μs delay in order to supply stop signals to the TAC module. The

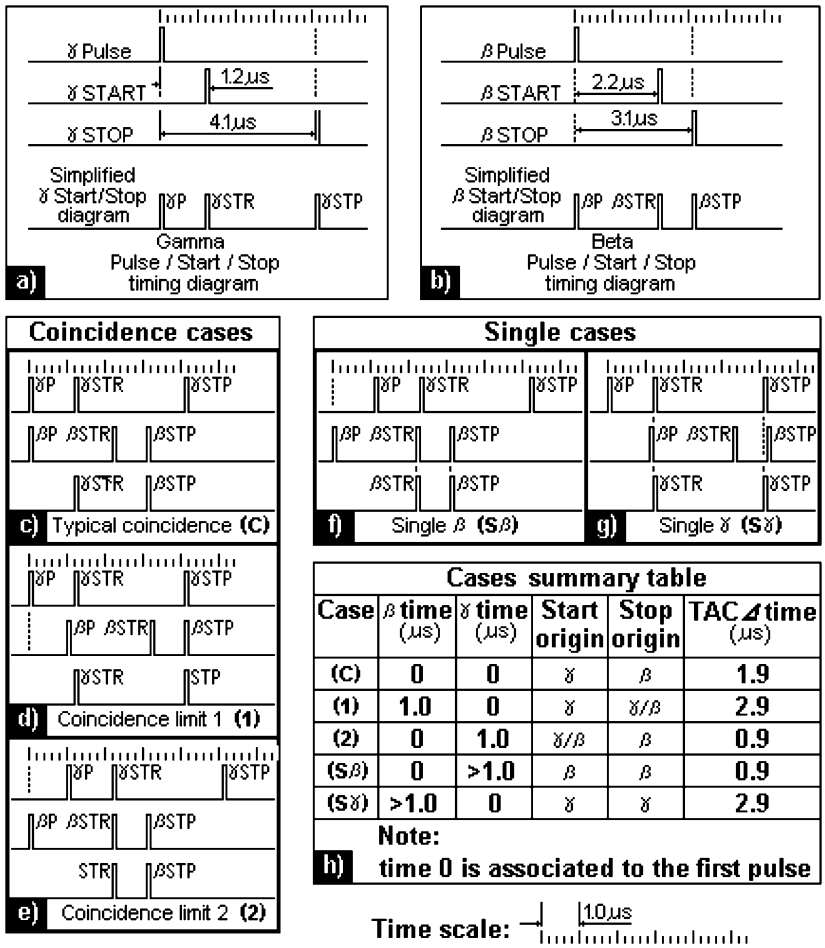

Fig. 5. Timing table of individual pulses from the electronic system. (a) and (b) show the TAC Start/Stop timing for gamma and beta lines respectively; (c) represents a typical coincidence when the beta and gamma pulses arrive simultaneously in the circuit; (d) represents a limiting coincidence case when the beta pulse occurs with a 1.0 μs delay relative to the gamma pulse occurrence; (e) represents the other limiting coincidence case when the gamma pulse occurs 1.0 μs after the beta pulse.

coincidence peak position in the TAC spectrum corresponds to the time difference between the β and γ SCA delay settings.

Fig. 5 explains the operation of the electronic system shown in Fig. 4, considering the main nominal delays given by the electronic modules. Fig. 5(a) and (b) show the TAC Start/Stop timing for gamma and beta lines respectively; the simplified diagrams at the bottom of these figures are used in the other sections of this figure. Sections c) to g) show the possible Start/Stop combinations; Section h) summarizes these combinations explained as follows: case c) represents a typical coincidence when the beta and gamma pulses arrive simultaneously in the circuit; here the Start is given by the gamma pulse and the Stop by the beta one, after a 1.9 μs delay; Section d) represents a limiting coincidence case when the beta pulse occurs with a 1.0 μs delay relative to the gamma pulse occurrence; thus, the Start is given by the gamma pulse and the Stop by both beta or gamma pulses, after a 2.9 μs delay; Section e) represents the other limiting coincidence case when the gamma pulse occurs 1.0 μs after the beta pulse; the Start can be given by both beta and gamma pulses; the beta pulse is responsible for the TAC Stop, after a 0.9 μs delay; If the relative delay of detection pulses exceeds 1.0 μs, the first arriving pulse - beta or gamma - is responsible for both Start and Stop TAC signals; no coincidence is considered by the system and the processed pulse is registered as a single; a single beta is added into the 0.9 μs time peak; a single gamma is added into the 2.9 μs time peak. According to the above explanation, the electronic system establishes a 2.0 μs coincidence range; so, a relative jitter between the beta and gamma detection pulses smaller than 1.0 μs is acceptable. Such a coincidence range is large enough to account for detection timing fluctuations and compensate different module propagation delays, enabling changes in these modules; also the accidental coincidences are distributed along this range.

Fig. 6 shows a timing diagram of pulses coming from each electronic module. The meaning of labels A to I are explained in Table I which includes the time of ocurrence and the dead time associated with each event. The amplifier output time was considered at maximum pulse amplitude. These dead time values for all modules were determined experimentally by means of a precision oscilloscope, except for the case of the MCA. The latter dead time was determined from live and clock times and checked by means of a precision pulser inserted in the TAC spectrum. Fig. 6(b) shows the Dead Time contribution of both the electronic system (labeled TAC for simplicity) and the Multi Channel Analyzer (MCA). The timing diagram in this section demonstrates that the effective dead time is equivalent to 15 μs

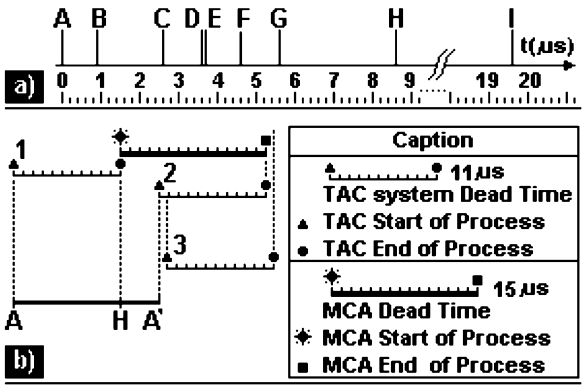

Fig. 6. Timing diagram of electronic system. (a) event time scale; the labels are explained in Table I; (b) dead time contribution from the electronic system (labeled TAC for simplicity) and from the Multi Channel Analyzer (MCA).

TABLE I
TIMING SIGNALS PRODUCED IN THE ELECTRONIC SYSTEM

Label	Event	Time (μs)	Dead Time (μs)
A	Disintegration	0	0
B	Output Amp. β and γ	0.9	1.8
C	Output SCA β	2.6	0.5
D	Output SCA γ	3.6	0.5
E	Output Gate and Delay G2	3.7	0.1
F	Output Delay Amp. β	4.6	1.0
G	Output Gate and Delay G1	5.6	3.0
H	Input TAC	8.6	11.0
I	Input MCA	19.6	15.0

(MCA typical Dead Time), explained as follows: a detection pulse arrives at instant labeled 1 and the TAC system starts the process, taking about 11 μs to generate the correspondent output signal; thus, the MCA starts its own process; any other detection pulse that arrives between the A-H time interval is neglected (instant 2 represents the extreme condition); although the TAC could accept a pulse inside the H-A' time interval, the correspondent TAC output would take place inside the MCA processing time; the pulse in the case 3 will be processed normally.

As can be seen from Fig. 6 and Table I, the dominant dead time comes from the MCA module. For this module the dead time is channel dependant and was determined experimentally, resulting in the range between 13.4 to 15.4 μs depending on the measurement conditions. A typical and most frequent value was about 15.0 μs.

A typical TAC spectrum registered in the MCA is shown in Fig. 7. The middle peak corresponds to coincidences. The left and right peaks correspond to beta and gamma counting rates, respectively, without the coincidence rate contribution. This electronic system allows experimental determination of the accidental coincidence contribution from the TAC spectrum. These events lie between the β or γ peaks and the coincidence peak. The coincidence time distribution has a FWHM (Full Width at Half Maximum) of 0.12 μs corresponding to $\pm$0.06 μs average time jitter, relative to the coincidence peak center. The coincidence peak is positioned at 2.4 μs, far enough from the

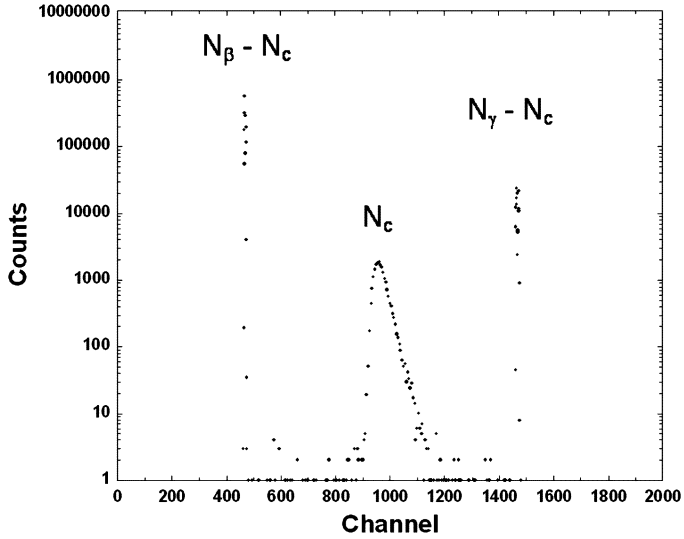

Fig. 7. Typical TAC output spectrum. The left peak corresponds to beta singles, excluding coincidences, the middle peak corresponds to coincidence counts and the right peak corresponds to gamma singles, excluding coincidences.

single gamma peak, located at 3.7 μs. This coincidence time shift is due to an intrinsic delay, about 0.6 μs, in the Gate and Delay modules, G1 and G2, not considered in Fig. 5.

As pointed out in section A, the minimum lower level discriminator set for the beta channel corresponds to 6 keV, well above the value of 3 keV given in [14] as the maximum amplitude for spurious afterpulses at 22 Celsius, which was the room temperature during the present experiment. Therefore, considering the beta discrimination and the dead time range of the electronic system, it can be concluded that the contribution from afterpulses can be considered negligible.

E. Source Preparation

A set of ten ^{18}F sources with masses in the 20–45 mg range were prepared by depositing quantitative aliquots of radioactive solutions onto a 20 μg.cm^{-2} thick Collodion film, previously coated with a 10 μg.cm^{-2} gold layer. This gold layer is not necessary for the plastic scintillator detection system and was applied only to allow comparisons with the conventional 4π proportional counter coincidence system. The accurate source mass determination was performed by the pycnometer technique [15] using a Mettler 5SA balance. The sources were dried under a red lamp. Immediately after measurement in the 4π proportional counter coincidence system, the ^{18}F sources were transferred to a stainless steel ring 0.1 mm thick, 20 mm in external diameter and 10 mm in internal diameter to be measured in the 4π plastic scintillator coincidence system.

F. Coincidence Equations

The value of source activity N_0 was derived for ^{18}F from the generalized coincidence formalism [2], as follows.

The number of beta counts is given by:

$$N_\beta = aN_o\epsilon_\beta + bN_o\epsilon_{\rm ec} + aN_o\left(1-\epsilon_\beta\right)\left(2\epsilon_{\beta\gamma} - \left(\epsilon_{\beta\gamma}\right)^2\right). \quad (1)$$

Where: N_β is the beta counting rate; a is the β^+ branching ratio; b is the electron capture branching ratio; ϵ_{ec} is the efficiency for electron capture events; $\epsilon_{\beta\gamma}$ is the annihilation gamma-ray efficiency of the beta detector. ϵ_β is the β^+ particles efficiency of the beta detector.

The detection efficiency for electron capture (ϵ_{ec}) in the PC system has been estimated by extrapolation of known values from ^{51}Cr, ^{54}Mn and ^{133}Ba coincidence measurements, and the result is presented in section G. For the PS system, this efficiency is nearly zero because the X-ray energy is only 0.53 keV and the Auger electron energy is only 0.456 keV. The corresponding pulses fall below the noise threshold. In this case,

$$N_\beta = aN_o\epsilon_\beta + aN_o(1-\epsilon_\beta)[2\epsilon_{\beta\gamma} - (\epsilon_{\beta\gamma})^2]. \quad (2)$$

The number of gamma counts is given by:

$$N_\gamma = aN_o\left(2\epsilon_\gamma - \epsilon_\gamma^2\right). \quad (3)$$

Where ϵ_γ is the gamma detector efficiency. The coincidence counts are given by:

$$N_c = aN_o\left(2\epsilon_\gamma - \epsilon_\gamma^2\right)\{\epsilon_\beta + (1-\epsilon_\beta)[2\epsilon_{\beta\gamma} - (\epsilon_{\beta\gamma})^2]\}. \quad (4)$$

The factor of 2 in (1), (2), (3) and (4) accounts for the two annihilation quanta emitted per β^+ transition. The quadratic term in (1) and (2) accounts for summing coincidences between annihilation quanta from a given pair, both detected in the beta detector.

Combining (2), (3) and (4), one obtains:

The gamma ray detector has been set to select only the total energy absorption peak. In this case, the possibility of having coincidence events coming from partial detection in the gamma detector must be removed from (4) and (5). Taking this effect into account (5) becomes [bottom of page]. After a few simplifications, (6) becomes [bottom of page]. The parameter

$$\left(\frac{1-N_c/N_\gamma}{N_c/N_\gamma}\right)$$

goes to zero when N_c/N_γ approaches unity. Since the latter parameter is a measure of ϵ_β, the left side of (7) [bottom of page] in this extrapolation limit gives the radioactive source activity. The slope given by the numerator is partially compensated by the denominator. As a result, the expected slope is small. Since the Auger electrons and X-rays have very low energy ($<$0.6 keV), it was estimated that their detection efficiencies approach zero. For this reason, the extrapolated value must be corrected for the β^+ branching ratio. Several measurements have been performed by moving the lower discrimination level in the beta channel, in order to change the efficiency. The activity and efficiency parameters were obtained using the CONTAC [16] code

$$\frac{N_\beta N_\gamma}{N_c} = \frac{aN_o\epsilon_\beta\left\{1+\frac{(1-\epsilon_\beta)}{\epsilon_\beta}\left[2\epsilon_{\beta\gamma}-(\epsilon_{\beta\gamma})^2\right]\right\}aN_o(2\epsilon_\gamma-\epsilon_\gamma^2)}{aN_o(2\epsilon_\gamma-\epsilon_\gamma^2)\left\{\epsilon_\beta+(1-\epsilon_\beta)\left[2\epsilon_{\beta\gamma}-(\epsilon_{\beta\gamma})^2\right]\right\}} \quad (5)$$

$$\frac{N_\beta N_\gamma}{N_c} = \frac{aN_o\epsilon_\beta\left\{1+\frac{(1-\epsilon_\beta)}{\epsilon_\beta}\left[2\epsilon_{\beta\gamma}-(\epsilon_{\beta\gamma})^2\right]\right\}aN_o(2\epsilon_\gamma-\epsilon_\gamma^2)}{aN_o\left\{\epsilon_\beta(2\epsilon_\gamma-\epsilon_\gamma^2)+2\epsilon_\gamma\epsilon_{\beta\gamma}(1-\epsilon_\beta)\right\}} \quad (6)$$

$$\frac{N_\beta N_\gamma}{Nc} = \frac{aN_o\left\{1+\frac{(1-\epsilon_\beta)}{\epsilon_\beta}\left[2\epsilon_{\beta\gamma}-(\epsilon_{\beta\gamma})^2\right]\right\}}{\left\{1+\frac{\epsilon_{\beta\gamma}}{\left(1-\frac{\epsilon_\gamma}{2}\right)}\frac{(1-\epsilon_\beta)}{\epsilon_\beta}\right\}} \quad (7)$$

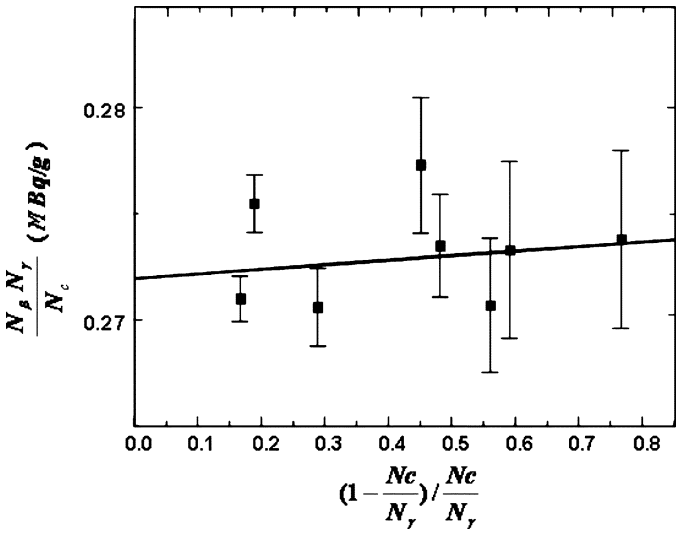

Fig. 8. Extrapolation curve of $N_\beta N_\gamma / N_c$ as a function of $((1 - N_c)/N_\gamma)/(N_c/N_\gamma)$ for ^{18}F. The correction for β^+ branching ratio was not included.

which performs corrections for decay, background, accidental coincidences and dead time. The dead time correction was estimated first by the values of MCA clock and live times. The accidental coincidences were then taken into account by applying the Cox-Isham formalism [6], [17] to N_c/N_γ parameter.

G. Results and Discussion

The source activity was obtained by linear least square fitting of $N_\beta N_\gamma / N_c$ as a function of $((1 - N_c)/N_\gamma) / (N_c/N_\gamma)$ using the LINFIT [18] code which incorporates covariance matrix methodology and takes into account all correlations involved [19]. Fig. 8 shows a plot of $N_\beta N_\gamma / N_c$ versus $((1 - N_c)/N_\gamma)/(N_c/N_\gamma)$ for ^{18}F. The resulting slope of the curve was (0.009 ± 0.015). This slope is zero within its uncertainty. The highest β^+ detection efficiency was around 85% for the $4\pi\beta(\mathrm{PS})$, whereas it reached about 96% for the $4\pi\beta(\mathrm{PC})$. Improvements in the system are planned in order to raise the PS efficiency. The activity result for the PS system was obtained by dividing the extrapolated value by the β^+ branching ratio. For the PC system the extrapolated value was corrected by the β^+ branching ratio and partial contribution of Electron Capture branching ratio, according to ϵ_{EC} value (estimated to be 0.25 ± 0.10). The results for the final activity per gram of radioactive solution obtained for PS and PC coincidence systems are shown in Table II. As can be seen both are in good agreement within the experimental uncertainty. The partial uncertainties involved are presented in Table III. The labels A and B stands for statistical and systematic errors, respectively, in accordance to the ISO Guide of Expression of Uncertainty in Measurement [20]. The uncertainty in the dead time correction was estimated by inserting a precision pulser in the middle of the TAC spectrum during a coincidence counting measurement and comparing the pulser peak area with the expected pulser rate. The main uncertainty component for the PC system is due to decay scheme branching ratio. This value was obtained by combining the uncertainty in PC electron capture efficiency and the uncertainty in the branching ratio taken from the literature [10]. This uncertainty is different from the other system because in the PS case the electron capture efficiency was estimated to be near zero. The total uncertainty was obtained by adding the partial uncertainties in quadrature. This overall uncertainty are comparable to those obtained in the NPL intercomparison [11] and can be considered satisfactory for calibrating secondary standard systems such as HPGe spectrometers and ionization chambers.

TABLE II
COMPARISON OF ACTIVITY VALUES OBTAINED WITH CONVENTIONAL $4\pi(\mathrm{PC})$ AND PRESENT $4\pi(\mathrm{PS})$ SYSTEMS

Radionuclide	System	Activity (MBq/g)
^{18}F	4π (PC)	0.2818 ± 0.0013
^{18}F	4π (PS)	0.2823 ± 0.0014

TABLE III
PARTIAL UNCERTAINTIES INVOLVED IN ACTIVITY DETERMINATION (IN PERCENT, AT 68% CONFIDENCE LEVEL). TYPES A AND B ARE STATISTICAL AND SYSTEMATIC ERRORS, RESPECTIVELY

Source of Error	Type of Error	$4\pi(PC)$	$4\pi(PS)$
Statistics per Data Point	A	0.092	0.41
Extrapolation Curve	A	0.23	0.30
Decay Correction	B	0.22	0.29
Decay Scheme	B	0.32	0.20
Mass	B	0.10	0.10
Dead Time	B	0.10	0.10
Total		0.47	0.51

III. CONCLUSION

The standardization of ^{18}F has been performed at a $4\pi(\mathrm{PS})\beta - \gamma$ coincidence system which makes use of plastic scintillators in 4π geometry. The results are in good agreement with respect to a conventional system and presented similar overall uncertainty. These results show that this new system can be used for the standardization of positron-emitter radionuclides by the coincidence method.

ACKNOWLEDGMENT

The authors are grateful to Mr. Maurício Marques for the sample preparations.

REFERENCES

[1] P. J. Campion, "The standardization of radioisotopes by beta-gamma coincidence method using high efficiency detectors," *Int. J. Appl. Radiat. Isot.*, vol. 4, pp. 232–248, 1959.
[2] A. P. Baerg, "Measurement of radioactivity disintegration rate by the coincidence method," *Metrologia*, vol. 2, no. 1, pp. 23–32, 1966.
[3] A. P. Baerg, "The efficiency extrapolation method in coincidence counting," *Nucl. Instrum. Methods*, vol. 112, pp. 143–150, 1973.
[4] M. F. Koskinas and M. S. Dias, "A coincidence system for radionuclide standardization using surface barrier detectors," *Nucl. Instrum. Methods Phys. Res. A*, vol. A280, pp. 327–331, 1989.

[5] K. A. Fonseca, M. F. Koskinas, and M. S. Dias, "Disintegration rate measurement of a ^{192}Ir solution," *Appl. Radiat. Isot.*, vol. 54, pp. 141–145, 2001.

[6] D. Smith, "Improved correction formulae for coincidence counting," *Nucl. Instrum. Methods*, vol. 152, pp. 505–519, 1978.

[7] L. Xiaoxia and W. Guojun, "Absolute radioactive measurement of ^{60}Co, ^{134}Cs and ^{166m}Ho by $4\pi\beta - \gamma$ anti-coincidence method," *Appl. Radiat. Isot.*, vol. 58, pp. 365–369, 2003.

[8] A. M. Baccarelli, M. S. Dias, and M. F. Koskinas, "Standardization of ^{241}Am by means of coincidence system using 4π plastic scintillator detector," in *Proc. 5th Regional Congress Radiation Protection and Safety*, Recife, Brazil, 2001, CD-ROM.

[9] A. M. Baccarelli, M. S. Dias, and M. F. Koskinas, "Coincidence system for standardization of radionuclides using a 4π plastic scintillator detector," *Appl. Radiat. Isot.*, vol. 58, pp. 239–244, 2003.

[10] F. Lagoutine, N. Coursol, and J. Legrand, "Table of radionucléides," Laboratoire de Metrologie des Rayonnements Ionisants, Bureau National de Metrologie, 1983.

[11] M. J. Woods and M. Baker, "Establishing equivalence for activity standards of short-lived radionuclides using NPL secondary standard radionuclide calibrator," *Appl. Radiat. Isot*, vol. 60, pp. 499–504, 2004.

[12] Y. Kawada, M. Ohtuka, Q. Wang, and Y. Hino, "Absolute radioactivity measurements by the use of a $4\pi\beta$-$4\pi\gamma$ detector configuration," *Appl. Radiat. Isot.*, vol. 60, pp. 357–362, 2004.

[13] F. Salvat, J. M. Fernandez-Varea, and J. Sempau, PENELOPE-2006, A Code System for Monte Carlo Simulation of Electron and Photon Transport, Rep. OECD ISBN 92-64-02301-1, 2006.

[14] Y. Kawada, M. Ohtuka, and Q. Wang, "Temperature dependence of spurious pulses in use of plastic scintillation detectors," *Appl. Radiat. Isot.*, vol. 60, pp. 403–407, 2004.

[15] P. J. Campion, "Procedures for accurately diluting and dispensing radioactive solutions," Bureau International des Poids et Mesures, Monographie BIPM-1, 1975.

[16] M. S. Dias, CONTAC: A Code for Activity Calculation Based on TAC Measurements IPEN-CNEN/SP, 2001, Internal Rep.

[17] D. R. Cox and V. Isham, "A bivariate point process connected with electronic counters," *Proc. Royal Society of London, Series A*, vol. 356, pp. 149–160, 1977.

[18] M. S. Dias, LINFIT: A Code for Linear Least Square Fit with Covariance Analysis IPEN-CNEN/SP, 1999, Internal Rep.

[19] D. L. Smith, *Probability, Statistics, and Ddata Uncertainties in Nuclear Science and Technology (Neutron Physics and Nuclear Data in Science and Technology)*. LaGrange Park, IL: American Nuclear Society, 1991.

[20] "Guide to the Expression of Uncertainty in Measurement," International Organization for Standardization, 1993.